


Article

A Visualization Experiment on Icing Characteristics of a Saline Water Droplet on the Surface of an Aluminum Plate

Yingwei Zhang, Xinpeng Zhou, Weihan Shi, Jiarui Chi, Yan Li * and Wenfeng Guo * 

College of Engineering, Northeast Agricultural University, Harbin 150030, China; zhangyingweineau@163.com (Y.Z.); neauzxp@163.com (X.Z.); a13114593518@163.com (W.S.); 17357711921@163.com (J.C.)

* Correspondence: liyanneau@163.com (Y.L.); guowenfengmail@163.com (W.G.)

Abstract: When the offshore device, such as an offshore wind turbine, works in winter, ice accretion often occurs on the blade surface, which affects the working performance. To explore the icing characteristics on a microscale, the freezing characteristics of a water droplet with salinity were tested in the present study. A self-developed icing device was used to record the icing process of a water droplet, and a water droplet with a volume of 5 μL was tested under different salinities and temperatures. The effects of salinity and temperature on the profile of the iced water droplet, such as the height and contact diameter, were analyzed. As the temperature was constant, along with the increase in salinity, the height of the iced water droplet first increased and then decreased, and the contact diameter decreased. The maximum height of the iced water droplet was 1.21 mm, and the minimum contact diameter was 3.67 mm. With the increase in salinity, the icing time of the water droplet increased, yet a minor effect occurred under low temperatures such as $-18\text{ }^{\circ}\text{C}$. Based on the experimental results, the profile of the iced water droplet was fitted using the polynomial method, with a coefficient of determination (R^2) higher than 0.99. Then the mathematical model of the volume of the iced water droplet was established. The volume of the iced water droplet decreased along with temperature and increased along with salinity. The largest volume was 4.1 mm^3 . The research findings provide a foundation for exploring the offshore device icing characteristics in depth.



Citation: Zhang, Y.; Zhou, X.; Shi, W.; Chi, J.; Li, Y.; Guo, W. A Visualization Experiment on Icing Characteristics of a Saline Water Droplet on the Surface of an Aluminum Plate. *Coatings* **2024**, *14*, 155. <https://doi.org/10.3390/coatings14020155>

Academic Editors: Ludmila B. Boinovich and Dariusz Bartkowski

Received: 5 December 2023

Revised: 19 January 2024

Accepted: 19 January 2024

Published: 23 January 2024



Copyright: © 2024 by the authors. Licensee MDPI, Basel, Switzerland. This article is an open access article distributed under the terms and conditions of the Creative Commons Attribution (CC BY) license (<https://creativecommons.org/licenses/by/4.0/>).

Keywords: offshore wind turbine; icing; water droplet; salinity; visualization test

1. Introduction

Wind energy is one of the most popular renewable energies around the world and is mainly used in the field of wind power [1]. The wind turbine realizes the conversion of wind energy into electric power without any pollution [2]. However, most high-quality wind energy resources are mainly located in the high-altitude and high-latitude regions [3]. In these regions, the temperatures were low in the winter. Therefore, when wind turbines work in such an environment, ice accretion often occurs on the blade surface. Under this condition, the aerodynamic profile of the blade is destroyed by ice. Then the aerodynamic characteristics of the blade degrade, and the power efficiency of the wind turbine decreases [4,5]. Additionally, icing results in an increase in mass and the destruction of the balance of the rotor, which affects the stability and lifespan of wind turbines. Under some extreme conditions, a shedding ice event also threatens the nearby buildings and staff.

Therefore, exploring the icing characteristics of wind turbines is necessary to ensure stability and power efficiency. With the rapid development of wind farms, onshore high-quality wind energy resources are gradually becoming scarcer. Thus, more and more offshore wind farms are being developed all over the world. For offshore wind turbines, an icing event is prone to presenting on the blade surface because the humidity in the offshore region is far higher than that in the onshore region. In comparison with liquid water icing, wind turbine icing has its own characteristics. Many scholars have conducted

research on wind turbine icing on the macroscale [6,7]. These research findings introduced macro-icing characteristics, including ice amount, ice shape, ice distribution, ice type, and so on. Nevertheless, the selection of icing conditions in this research was decided according to the working conditions of onshore wind turbines [8,9]. The water droplets used in the air flow were pure water. In contrast, the working conditions of offshore wind turbines are significantly different from those of onshore wind turbines [10,11]. In addition to the difference in humidity, the composition of water droplets is also different. For the onshore wind turbine icing, the water droplets in the air are pure water vapor from freshwater. In contrast, for the offshore wind turbine icing, the water droplets in the airflow contain salts from sea water. For this reason, the icing characteristic between the onshore wind turbine and the offshore one is different. Therefore, it is necessary to explore offshore wind turbine icing, especially. At present, few experimental conditions have been selected based on the working conditions of offshore wind turbines [12,13]. Moreover, the research methods include the analytical method, simulation method, and experimental method [14,15]. In addition, the wind turbine icing also has micro-icing characteristics. The formation of ice on the macroscale stems from the water droplets flowing in the air and impacting the cold blade surface. Therefore, the micro-icing characteristics of water droplets also need to be explored, which could disclose the mechanism of wind turbine icing. In the previous research findings [16–20], the freezing process of a pure water droplet has been conducted on a metal surface under different icing conditions, such as temperature, water droplet volume, surface characteristics of the substrate, and so on. In comparison, the freezing characteristics of water droplets with salinity have been less studied [21–23], especially for the ingredients of sea water. Scholars examined the freezing characteristics of salty water droplets on the superhydrophobic surface, such as freezing time, contact angle, ice nucleation propagation, and so on.

In summary, macro- and micro-icing characteristics are both important to wind turbine icing. Previous explorations in these two aspects both provide valuable experience and research methods for carrying out the present study. In the present study, the freezing process and characteristics of a water droplet with the ingredient of sea water were tested. An experimental system with a freezing part and an image acquisition part was developed. The freezing process of the water droplet was recorded and processed. The effect of salinity on the icing characteristics of the water droplet was analyzed, including the height, contact diameter, and icing time of the water droplet. And the profile of a frozen water droplet was regressed by the polynomial method. The research findings provide a basis for exploring the macro-icing characteristics of an offshore wind turbine.

2. Experimental Scheme and System

In the present study, the freezing characteristics of water droplets under different salinities were tested. The experimental scheme was listed in Table 1.

Table 1. Experimental scheme.

Items	Values
Volume of water droplet	5 μ L
Substrate temperatures	−6 °C, −12 °C, −18 °C
Salinities of water droplets	0 g/L, 6 g/L, 12 g/L, 18 g/L, 26.7 g/L
Substrate material	Aluminum

As listed in Table 1, the volume of the water droplet was 5 μ L, and three kinds of temperatures were selected in the present study. The temperatures were decided according to the ice types of the wind turbines. When the temperature is high, the ice type is glaze ice. On the contrary, the ice type is rime ice in low-temperature conditions. In medium temperatures, the ice type is mixed ice [24]. For the salinity, five kinds were determined, which were measured and selected according to the salinity of the Bohai Sea in China. The Bohai Sea is located in the north of China. The lowest temperature was approximated

at $-20\text{ }^{\circ}\text{C}$. To make real sea water as much as possible, sea salt and pure water were used according to the measurement results. Additionally, aluminum was selected as a precooling substrate for contact with a water droplet. The reason for the selection is that aluminum has the characteristics of high and isotropic heat conductivity, which is widely used by many scholars. In addition, some small-scale wind turbine blades are made of aluminum material.

For carrying out the icing tests of a water droplet based on the experimental scheme, an icing system was designed and built in the present study. The diagrammatic sketch is shown in Figure 1.

As shown in Figure 1, the experimental system is mainly composed of a freezing device, an industrial camera, a DC power supply, a chiller, a micro-pump, a computer, and so on. The freezing device was a closed chamber that was made of acrylic material because of its better transparency for capturing images. It was used to realize the freezing process of water droplets. The Peltier element (12710) was used as the freezing component in the freezing device. It has the advantages of a small scale, no noise, no vibration, a stable temperature, and low power consumption. In the present study, three pieces were used. One piece was used to cool the substrate, and the other two were used to cool the space over the substrate in the freezing device. The cooling substrate was a core component that was adhered between an aluminum block for dissipating heat and a copper base for the cooling substrate. When it works, one side is used to freeze the copper base, and the other side, which generates heat, is cooled by the aluminum block. The chiller (JZ-5200, JIZHI Electromechanical Co., Ltd. Guangzhou in China) circulates the cooling water flowing through the aluminum block. The aluminum substrate for water droplet icing was located on the copper base. The water droplet was injected out of a syringe by a micro-pump (LSP02-2A, LONGER Co., Ltd., Baoding, China). The moving resolution of it is $0.03125\text{ }\mu\text{m}$. The industrial camera (XG1205GC-T, MindVision Technology Co., Ltd., Shenzhen, China) was used to record the freezing process of the water droplet. The visual range of the lens is $4\text{ mm} \times 3.2\text{ mm}$, and the image resolution is 4096×3072 . After the test, the image of the iced water droplet profile was processed by image processing software (Photoshop 2023).

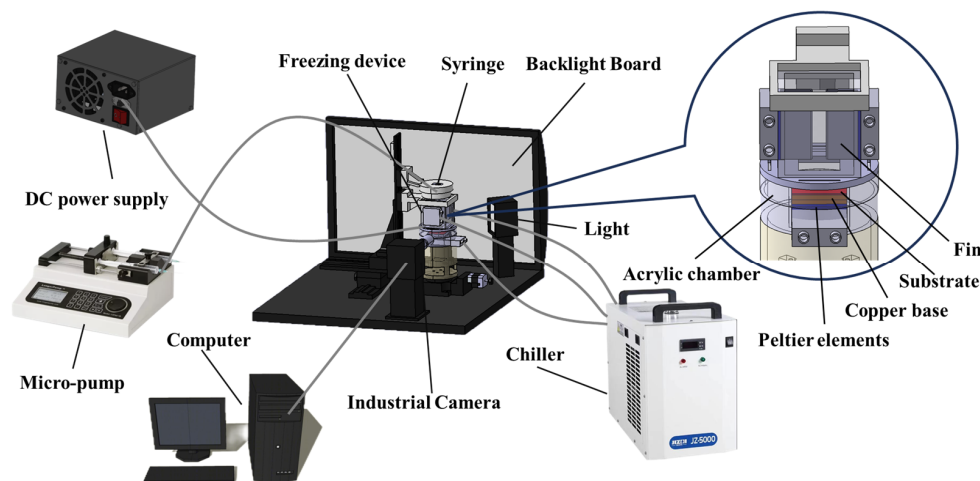


Figure 1. Schematic diagram of experimental system.

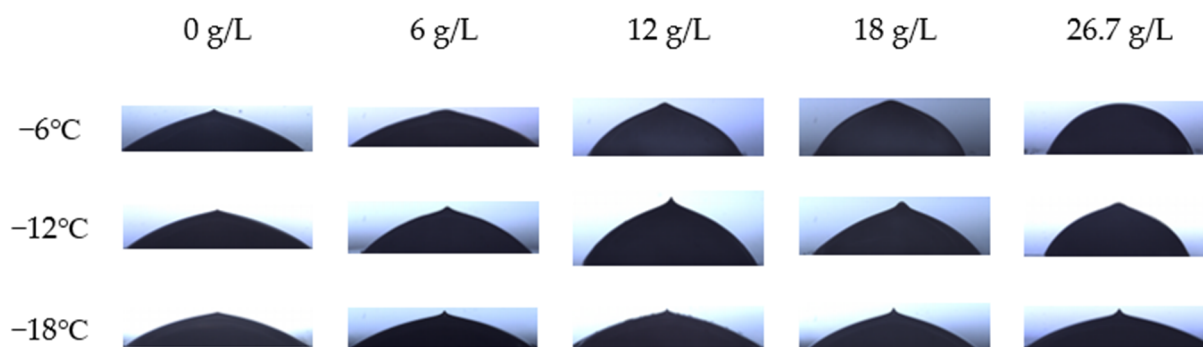
3. Experimental Results

According to the experimental scheme, icing tests of water droplets on the aluminum plate surface were carried out. An aluminum plate (1060, CHINALCO SOUTHWEST ALUMINUM GROUP, Chongqing, China) with a size of $40\text{ mm} \times 40\text{ mm} \times 1\text{ mm}$ was used as the substrate. The thickness of the aluminum plate is 2 mm , and the surface roughness R_a is $0.17\text{ }\mu\text{m}$. For exploring the freezing process of sea water, sea salt was used to make a saline solution in the present study. The key ingredients in the saline solution are listed in Table 2.

Table 2. Key ingredients of sea salt.

Ingredients	Concentration (mg/L)
Na ⁺	9500~10,500
Cl ⁻	16,500~18,500
SO ₄ ²⁻	2000~2600
Mg ²⁺	950~1400
K ⁺	280~380
Ca ²⁺	300~420

In the present study, a thermocouple temperature sensor (TT-K-36) was used to monitor the substrate temperature. Before experiments, the temperatures over the substrate were measured when the substrate temperatures were $-6\text{ }^{\circ}\text{C}$, $-12\text{ }^{\circ}\text{C}$, and $-18\text{ }^{\circ}\text{C}$, respectively. The measurements show that the temperature over the substrate was $2\text{ }^{\circ}\text{C}\sim 4\text{ }^{\circ}\text{C}$ lower than the one on the substrate surface. It satisfied the requirement of a low-temperature environment. The water droplet was injected from the syringe and fell onto the aluminum plate surface with an approximate velocity of 1 m/s. Before each test, the aluminum plate was cleaned with deionized water in an ultrasonic cleaning machine. Then it was dried by hot air. After that, it was placed in the freezing device and precooled to the experimental temperature. The icing results under different salinities and temperatures are shown in Figure 2.

**Figure 2.** Results of iced water droplets under different salinities and temperatures.

As shown in Figure 2, when the temperature was high, such as $-6\text{ }^{\circ}\text{C}$, the salinity had a significant effect on the profile of the iced water droplet. Under low-salinity conditions, the contact angle of the iced water droplet was low and generated a tip on the top after freezing. On the contrary, the contact angle increased along with salinity, and the tip disappeared. In contrast, when the temperature was low, such as $-18\text{ }^{\circ}\text{C}$, the effect of salinity became insignificant. The contact angles were small, and there were tips under all salinity conditions. This phenomenon resulted from the brine rejection effect [25]. In the process of freezing the water droplet with salinity, the salt ions were rejected from the frozen part into the unfrozen part. It led to an increase in salinity in the unfrozen part [26–28]. This effect increased the concentration and surface tension and gradually decreased the freezing point of the unfrozen solution. Meanwhile, the icing time of the water droplet was delayed, the volume expansion was slight, and there might have been a little unfrozen salty water at the top of the water droplet. In this case, tip disappearance was observed at last. In the present study, when the temperature was high, such as $-6\text{ }^{\circ}\text{C}$, the freezing process was slow, and there was enough time to reject salt ions from the frozen part into an unfrozen one in a water droplet, which resulted in tip disappearance. In contrast, with the decrease in temperature, such as $-12\text{ }^{\circ}\text{C}$ and $-18\text{ }^{\circ}\text{C}$, the freezing time shortened, and the salt ions in the frozen part could not diffuse into the unfrozen part instantly. For this reason, the freezing rate was high, and the volume expansion effect was obvious at the

tip of the water droplet, which led to the tip generation at last. However, even at a low temperature, the brine rejection effect still existed in the freezing process.

Based on the icing test, the images of iced water droplets were processed, and the profiles are shown in Figure 3.

As shown in Figure 3, according to the processing results, the profiles of iced water droplets can be quantitatively analyzed, which will be discussed in the next sections.

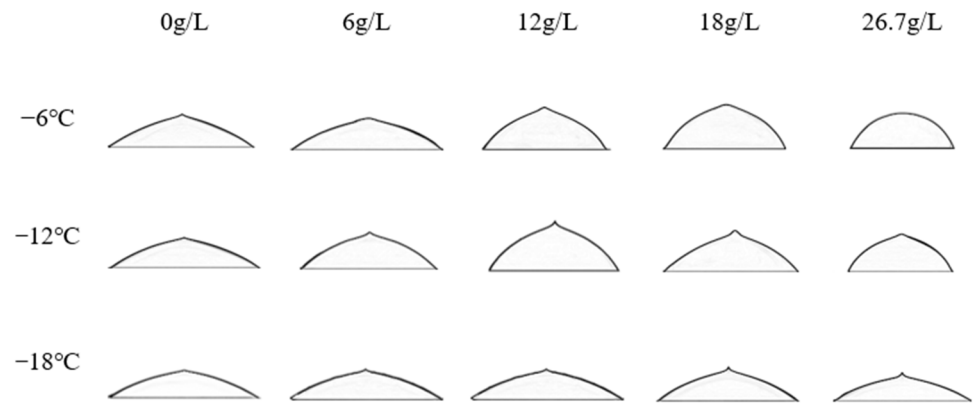


Figure 3. Profiles of iced water droplets under different salinities and temperatures.

4. Discussion and Analysis

Based on the icing tests and image processing results, the effect of salinity on the profile of iced water droplets was analyzed, including the height h and contact diameter d of the iced water droplet, which are shown in Figure 4.

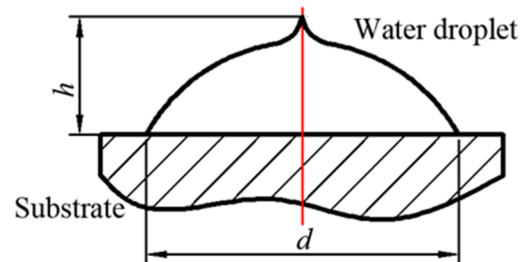


Figure 4. Schematic profile of an iced water droplet.

4.1. Effect of Salinity on Height of Iced Water Droplet

The variation in height of the iced water droplet with salinity is shown in Figure 5. As shown in Figure 5, salinity has a significant effect on the height of the iced water droplet. When the temperature was constant, the height of the iced water droplet increased first. The reason for this result is that salinity affects the surface tension of water droplets. The surface tension of salty water increases along with salinity [29]. Therefore, in comparison with the water droplet without salinity, the one with salinity had a higher surface tension to make the surface of the water droplet contract tightly, which resulted in an increase in the height of water droplet. However, as shown in Figure 5, when the salinity is too high, such as 26.7 g/L, the increase in height was not obvious and even somewhat decreased. As discussed in Section 2, the brine rejection effect decreases the freezing point of a water droplet in the freezing process. Then the icing time increased and the water droplet flew peripherally, which resulted in a decrease in height and tip disappearance. Additionally, at a high temperature, such as $-6\text{ }^{\circ}\text{C}$, the variation in height is a little different from the ones at low temperatures of $-12\text{ }^{\circ}\text{C}$ and $-18\text{ }^{\circ}\text{C}$. When the salinity was low, the height decreased first and then increased. The reason for this difference is that low salinity has little effect on the surface tension of water droplets. After contact with the substrate, the water droplet did not freeze in a short time and flew peripherally under a high temperature.

It resulted in a decrease in the height of the iced water droplet. With the increase in the salinity, the rule of variation was the same for the ones at low temperatures of $-12\text{ }^{\circ}\text{C}$ and $-18\text{ }^{\circ}\text{C}$.

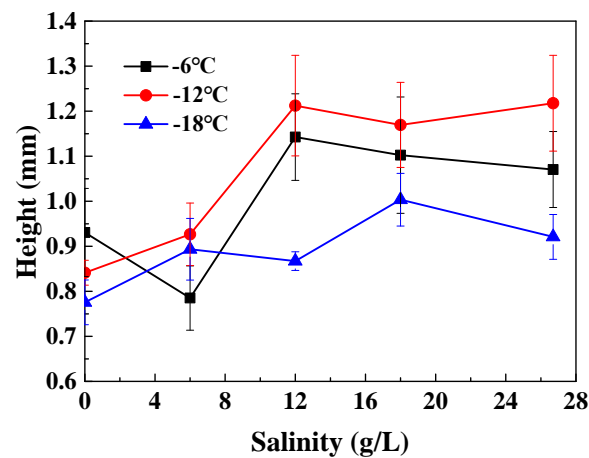


Figure 5. Variation in the height of iced water droplet with salinity.

In addition, from Figure 5, as the salinity was constant, the height of the iced water droplet at $-12\text{ }^{\circ}\text{C}$ was the highest, the one at $-18\text{ }^{\circ}\text{C}$ was the lowest, and the one at $-6\text{ }^{\circ}\text{C}$ was medium. In comparison with the conditions between $-6\text{ }^{\circ}\text{C}$ and $-12\text{ }^{\circ}\text{C}$ the lower the temperature was, the higher the height of the iced water droplet was. The reason was that the icing time of the water droplet decreased along with temperature. In this case, the flowability of the water droplet decreased with the decrease in temperature. The water droplet was frozen in a shorter time, which resulted in an increase in the height of the water droplet. In contrast, when the temperature decreased further, such as $-18\text{ }^{\circ}\text{C}$, the height decreased again. The reason for this result is that the thickness of frost generating on the cold blade surface increased with the decrease in temperature [30]. In the tests, it was found that there was frost generated on the cold blade surface. At low temperatures, such as $-18\text{ }^{\circ}\text{C}$, the thickness of the frost was higher than the that in the conditions of $-6\text{ }^{\circ}\text{C}$ and $-12\text{ }^{\circ}\text{C}$. In this case, the thick frost layer isolated the cold substrate surface absolutely. Under this condition, the water droplet could not make contact with the substrate surface directly but rather the frost layer. After that, the heat transfer between the substrate and water droplet was conducted via the frost layer. For this reason, the frost began melting into water, which merged into a water droplet. The melted water film on the substrate surface intensified the flowability of the water droplet and decreased the concentration of salt in the water droplet, which increased the the contact diameter, decreased the height, and shortened the icing time of the water droplet. In contrast, when the temperature was high, such as $-6\text{ }^{\circ}\text{C}$ or $-12\text{ }^{\circ}\text{C}$, the frost layer was thin, and the effect of melted water film on the flowability of the water droplet was weak. That is why the height of the iced water droplet was higher than the one at a low temperature.

4.2. Effect of Salinity on Contact Diameter of Iced Water Droplet

The variation in contact diameter with salinity is shown in Figure 6. As shown in Figure 6, both salinity and temperature have significant effects on the contact diameter of the iced water droplet. Under non-salinity conditions, the effect of temperature on the contact diameter is slight. The contact diameters under different temperature conditions were approximate. With the increase in salinity, the discrepancies among different temperatures became obvious. When the temperature was high, such as $-6\text{ }^{\circ}\text{C}$ and $-12\text{ }^{\circ}\text{C}$, the contact diameter decreased with the increase in salinity. However, as the temperature was low, such as $-18\text{ }^{\circ}\text{C}$, the contact diameter varied little with the increase in salinity.

The reasons for the variations are that the icing process of the water droplet was affected by frost generation and heat transfer rate together. At a temperature of $-18\text{ }^{\circ}\text{C}$,

the thickness of the frost layer generated on the substrate surface and the heat transfer rate between the water droplet and substrate were both high. As discussed in Section 4.1, the thick frost layer increased the flowability of the water droplet after melting. That is why the contact diameter was larger than the ones under the temperatures of $-6\text{ }^{\circ}\text{C}$ and $-12\text{ }^{\circ}\text{C}$. Additionally, the high heat transfer rate under low-temperature conditions resulted in a decrease in the flowability of the water droplet after impacting on the substrate surface, which led to slight variation under different salinities.

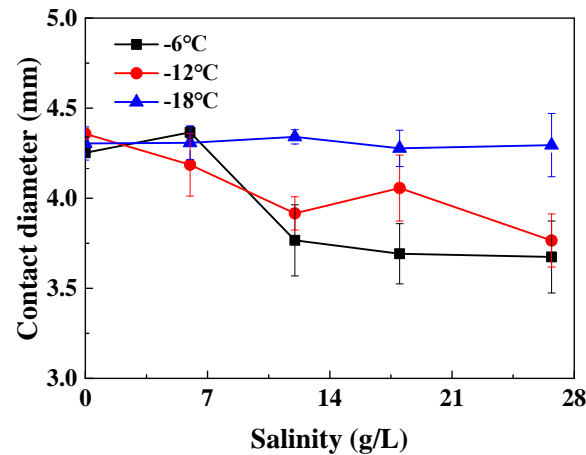


Figure 6. Variation of the contact diameter with salinity.

In contrast, at a temperature of $-6\text{ }^{\circ}\text{C}$ or $-12\text{ }^{\circ}\text{C}$, the flowability of the water droplet and the heat transfer rate were low in comparison with those at a temperature of $-18\text{ }^{\circ}\text{C}$, which resulted in a decrease in the contact diameter. Nevertheless, the surface tension of the water droplet increased along with salinity, as discussed above. Then the contact diameter decreased. The higher the salinity, the smaller the contact diameter. Especially at a temperature of $-6\text{ }^{\circ}\text{C}$, the contact diameter under low salinity increased first and then decreased. It shows that the surface tension has a smaller effect on contact diameter under low-salinity conditions. The decrease in freezing point had a significant effect, which resulted in an increase in contact diameter. In the condition of high salinity, surface tension played a key role in decreasing the contact diameter.

4.3. Effect of Salinity on Icing Time of Water Droplet

Similarly, the effect of salinity on the icing time of the water droplet was also analyzed, as shown in Figure 7.

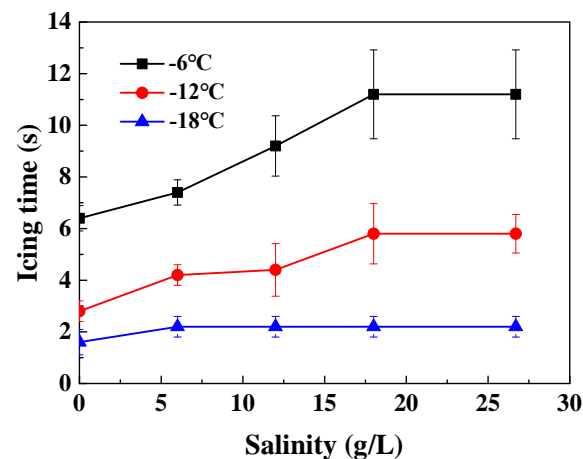


Figure 7. Variation of the icing time of water droplet with salinity.

As shown in Figure 7, the icing time of the water droplet increases along with salinity as the temperature is constant. The reason for this is that salinity decreases the freezing point of the water droplet. The higher the salinity, the lower the freezing point. Therefore, the icing time increased along with salinity. From Figure 7, when the temperature is high, such as $-6\text{ }^{\circ}\text{C}$ and $-12\text{ }^{\circ}\text{C}$, the icing time increases dramatically at first. As the salinity is higher than 18 g/L , the salinity has little effect on the icing time. It validates that with the increase in salinity; the freezing point of the water droplet decreased dramatically first and then slightly. It is also the same as previous research findings [31]. However, under low-temperature conditions, such as $-18\text{ }^{\circ}\text{C}$, salinity has little effect on the icing time of the water droplet. The icing time of the water droplet with salinity was just a little higher than that of the water droplet without salinity. It shows that a low temperature increases the heat transfer rate and shortens the icing time of water droplets.

4.4. Effect of Salinity on Profile of Iced Water Droplet

Based on the experimental results of the water droplet with salinity, the profiles of iced water droplets under different icing conditions were processed, which are shown in Figure 3. For analyzing the effect of salinity on the profile quantitatively, the processed profile of an iced water droplet is located in a coordinate, the contact interface between the water droplet and substrate was selected as an abscissa or x axis, and the leftmost point of the contact diameter was selected as the origin.

According to the image of the iced water droplet, some key points along the profile of the iced water droplet were selected to characterize the profile. For these points, the abscissa values were isometric along the contact diameter. In this way, the profile of an iced water droplet can be characterized quantitatively. Therefore, the profiles of iced water droplets under different salinities and temperatures are shown in Figures 8–10.

As shown in Figures 8–10, the profiles of iced water droplets were reconstructed in the coordinates. Then, based on the profile parameters, the profile was fitted by the polynomial method. The power of each fitting profile was decided according to the coefficient of determination R^2 . In the present study, the value of R^2 under each condition should be higher than 0.99. According to the criteria, the mathematical expressions of the fitting profiles are listed in Table 3. The fitting results coincide well with the experimental data.

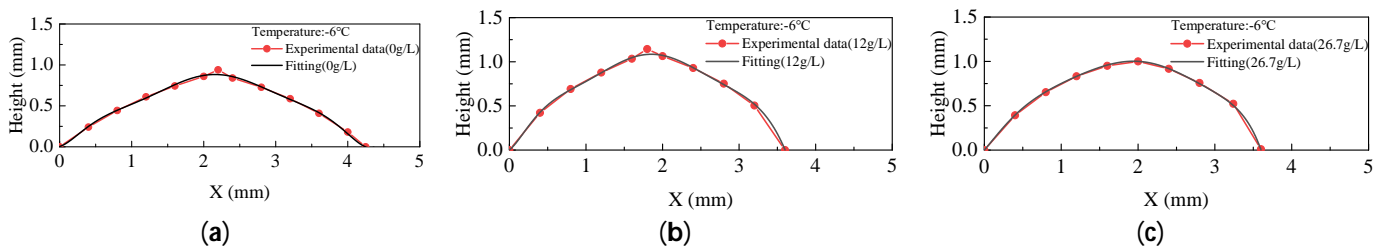


Figure 8. Fitting profiles of iced water droplets at the temperature of $-6\text{ }^{\circ}\text{C}$: (a) 0 g/L ; (b) 12 g/L ; (c) 26.7 g/L .

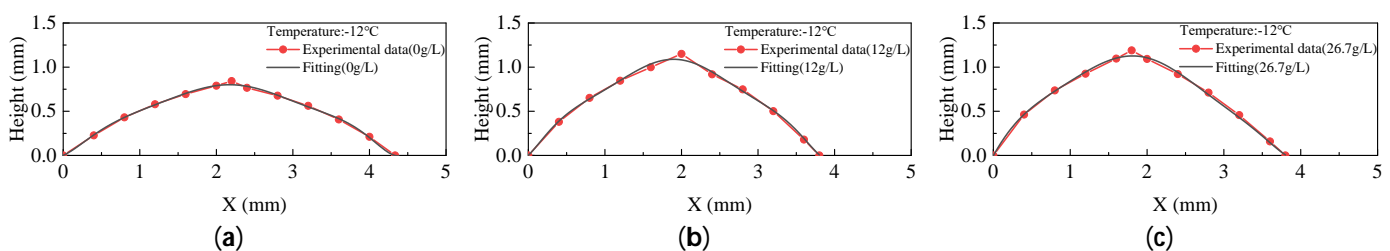


Figure 9. Fitting profiles of iced water droplets at the temperature of $-12\text{ }^{\circ}\text{C}$: (a) 0 g/L ; (b) 12 g/L ; (c) 26.7 g/L .

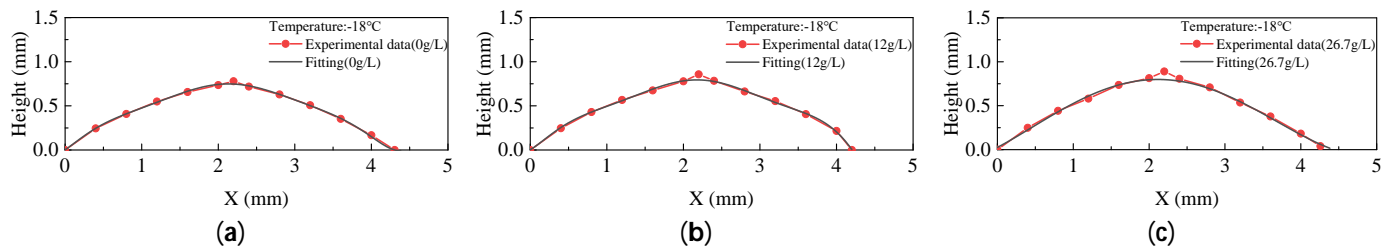


Figure 10. Fitting profiles of iced water droplets at the temperature of $-18\text{ }^{\circ}\text{C}$: (a) 0 g/L ; (b) 12 g/L ; (c) 26.7 g/L .

Table 3. Mathematical expressions of profile fitted by polynomial method.

Temperature	Salinity	Polynomial Equation	Coefficient of Determination
$-6\text{ }^{\circ}\text{C}$	0 g/L	$y = -0.1839x^2 + 0.7892x - 0.0351$	$R^2 = 0.9914$
	12 g/L	$y = 0.0211x^4 - 0.1387x^3 - 0.017x^2 + 0.9263x + 0.0203$	$R^2 = 0.9939$
	26.7 g/L	$y = 0.0191x^3 - 0.3626x^2 + 1.1348x - 0.011$	$R^2 = 0.9911$
$-12\text{ }^{\circ}\text{C}$	0 g/L	$y = -0.163x^2 + 0.7083x - 0.0174$	$R^2 = 0.9954$
	12 g/L	$y = 0.0273x^4 - 0.1947x^3 + 0.1434x^2 + 0.7851x + 0.017$	$R^2 = 0.9939$
	26.7 g/L	$y = 0.0291x^4 - 0.1821x^3 + 0.0125x^2 + 0.994x + 0.0216$	$R^2 = 0.9956$
$-18\text{ }^{\circ}\text{C}$	0 g/L	$y = -0.1542x^2 + 0.6599x - 0.003$	$R^2 = 0.9948$
	12 g/L	$y = -0.1575x^2 + 0.6843x - 0.0063$	$R^2 = 0.9961$
	26.7 g/L	$y = -0.1681x^2 + 0.717x - 0.0105$	$R^2 = 0.9918$

x (mm) is the position coordinate along contact diameter; y (mm) is the height of iced water droplet; R^2 is the coefficient of determination.

According to the mathematical expressions in Table 2, the volumes of iced water droplets were calculated in the present study for analyzing the effect of salinity on the volume of iced water droplets quantitatively. The schematic diagram of calculation method is shown in Figure 11.

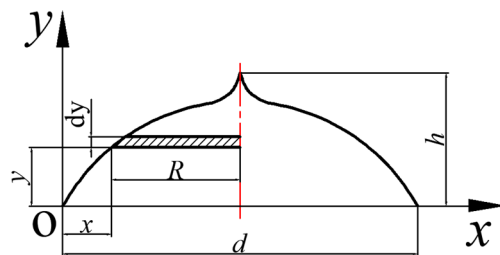


Figure 11. Model of the volume of an iced water droplet.

As shown in Figure 11, an infinitesimal element dy was selected at any point along the profile of an iced water droplet. The coordinates at this point are considered (x, y) , and the radius of the iced water droplet at this point is R , which is equal to the difference between the half-contact diameter $d/2$ and the coordinate x . Therefore, the infinitesimal volume of the iced water droplet is expressed in Equation (1).

$$dV = \pi\left(\frac{d}{2} - x\right)^2 \cdot dy \tag{1}$$

Then the whole volume of the iced water droplet is expressed as Equation (2).

$$V = \int_0^h \pi\left(\frac{d}{2} - x\right)^2 \cdot dy \tag{2}$$

Combining Equation (2) with Table 3, the volume of the iced water droplet can be calculated theoretically. The formation of dy and the scope of x under different conditions are listed in Table 4.

Table 4. Formation of dy and scope of x under different conditions.

Temperature	Salinity (g/L)	dy/dx	$d/2$ (mm)	x
−6 °C	0	$dy/dx = -0.3678x + 0.7892$	2.1	[0.0449, 4.2465]
	12	$dy/dx = 0.0844x^3 - 0.4161x^2 - 0.034x + 0.9263$	1.99	[−0.0219, 3.9549]
	26.7	$dy/dx = 0.0573x^2 - 0.3626x^2 + 1.1348x - 0.011$	1.96	[0.0097, 3.9394]
−12 °C	0	$dy/dx = -0.326x + 0.7083$	2.15	[0.0247, 4.3207]
	12	$dy/dx = 0.1092x^3 - 0.5841x^2 + 0.2868x + 0.7851$	1.99	[−0.0217, 3.9545]
	26.7	$dy/dx = 0.1164x^3 - 0.5463x^2 + 0.025x + 0.994$	1.99	[−0.0217, 3.9669]
−18 °C	0	$dy/dx = -0.3084x + 0.6599$	2.14	[0.0046, 4.275]
	12	$dy/dx = -0.315x + 0.6843$	2.16	[0.0092, 4.3355]
	26.7	$dy/dx = -0.3362x + 0.717$	2.12	[0.0147, 4.2506]

The variations in volumes with salinity under different temperatures are shown in Figure 12.

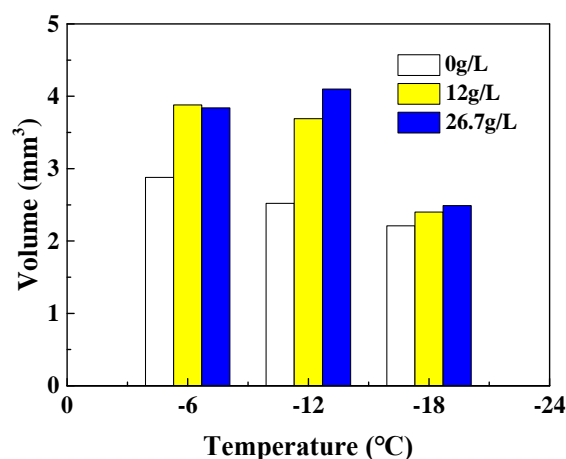


Figure 12. Variations in the volumes of iced water droplets with salinity and temperature.

As shown in Figure 12, both the salinity and the temperature have effects on the volume of iced water droplets. When the temperature was constant, the volume of an iced water droplet with salinity was higher than one without salinity. In contrast, for a salty water droplet, the effect of salinity on the volume was slight. However, as the salinity was constant, the volume decreased along with the temperature. For the low-temperature conditions, such as −18 °C, the volumes among all salinity conditions were approximate. It validates that the salinity had little effect on the volume of water droplet in the process of a phase change.

5. Conclusions

In the present study, the freezing characteristics of a water droplet with salinity were studied, and the effect of salinity on the profile of an iced water droplet was analyzed. Some conclusions were obtained and listed as follows:

1. The effects of salinity and temperature on the height of the iced water droplet have been explored. As the temperature was constant, the height of an iced water droplet increased dramatically first because of the increase in surface tension. In contrast, under high-salinity conditions, the increment decreased. In addition, as the temperature was low, the height decreased because there was thicker frost generated on the cold

surface, which led to an increase in the flowability of a water droplet after melting due to heat transfer.

2. The effects of salinity and temperature on the contact diameter of an iced water droplet have also been analyzed. Generally, the contact diameter of an iced water droplet decreased along with the increase in salinity because of the high surface tension of the salty solution. However, for low-temperature conditions, salinity had little effect on the contact diameter because of the increase in frost generation, which increases the flowability of water droplets after melting during heat transfer between the substrate and the water droplet.
3. The profile of an iced water droplet was obtained from the processing image. Based on the data, the fitting profile of an iced water droplet was also given by the polynomial method in a mathematical expression. The power of each polynomial expression under different conditions was decided according to the coefficient of determination. The fitting results coincide well with the experimental data. Based on the fitting results, the volumes of iced water droplets were also calculated by a mathematical model established in the present study. It validates that the volume decreased along with temperature and increased along with salinity.

Author Contributions: Conceptualization, Y.L. and W.G.; methodology, Y.Z.; software, X.Z.; validation, X.Z., W.S. and J.C.; formal analysis, W.G.; investigation, Y.Z.; resources, Y.L. and Y.Z.; data curation, X.Z. and W.G.; writing—original draft preparation, Y.Z.; writing—review and editing, Y.L. and W.G.; visualization, Y.Z.; supervision, Y.L.; project administration, W.G.; funding acquisition, W.G. All authors have read and agreed to the published version of the manuscript.

Funding: This research was funded by the Key Laboratory of Icing and Anti/De-icing of CARDC (Grant No. IADL 20220109).

Institutional Review Board Statement: Not applicable.

Informed Consent Statement: Not applicable.

Data Availability Statement: The data presented in this study are available on request from the corresponding author.

Conflicts of Interest: The authors declare no conflicts of interest.

References

1. Nwaigwe, K.N. Assessment of wind energy technology adoption, application and utilization: A critical review. *Int. J. Environ. Sci. Technol.* **2022**, *19*, 4525–4536. [[CrossRef](#)]
2. Balat, M. A Review of Modern Wind Turbine Technology. *Energy Sources Part A* **2009**, *31*, 1561–1572. [[CrossRef](#)]
3. Farina, A.; Anctil, A. Material consumption and environmental impact of wind turbines in the USA and globally. *Resour. Conserv. Recycl.* **2022**, *176*, 105938. [[CrossRef](#)]
4. Dalili, N.; Edrisy, A.; Carriveau, R. A review of surface engineering issues critical to wind turbine performance. *Renew. Sustain. Energy Rev.* **2009**, *13*, 428–438. [[CrossRef](#)]
5. Liu, Z.; Zhang, Y.; Li, Y. Superhydrophobic coating for blade surface ice-phobic properties of wind turbines: A review. *Prog. Org. Coat.* **2024**, *187*, 108145. [[CrossRef](#)]
6. Gao, L.; Liu, Y.; Hu, H. An experimental investigation of dynamic ice accretion process on a wind turbine airfoil model considering various icing conditions. *Int. J. Heat Mass Transf.* **2019**, *133*, 930–939. [[CrossRef](#)]
7. Yang, X.; Bai, X.; Cao, H. Influence analysis of rime icing on aerodynamic performance and output power of offshore floating wind turbine. *Ocean Eng.* **2022**, *258*, 111725. [[CrossRef](#)]
8. Shu, L.; Liang, J.; Hu, Q.; Jiang, X.; Ren, X.; Qiu, G. Study on small wind turbine icing and its performance. *Cold Reg. Sci. Technol.* **2017**, *134*, 11–19. [[CrossRef](#)]
9. Yi, X.; Wang, K.C.; Ma, H.L.; Zhu, G. Computation of icing and its effect of horizontal axis wind turbine. *Acta Energetica Sol. Sin.* **2014**, *35*, 1052–1058. (In Chinese)
10. Li, J.; Wang, G.; Li, Z.; Yang, S.; Chong, W.T.; Xiang, X. A review on development of offshore wind energy conversion system. *Int. J. Energy Res.* **2020**, *44*, 9283–9297. [[CrossRef](#)]
11. Cao, H.Q.; Bai, X.; Ma, X.D.; Yin, Q.; Yang, X.Y. Numerical Simulation of Icing on Nrel 5-MW Reference Offshore Wind Turbine Blades Under Different Icing Conditions. *China Ocean Eng.* **2022**, *36*, 767–780. [[CrossRef](#)]
12. Mu, Z.; Li, Y.; Guo, W.; Shen, H.; Tagawa, K. An Experimental Study on Adhesion Strength of Offshore Atmospheric Icing on a Wind Turbine Blade Airfoil. *Coatings* **2023**, *13*, 164. [[CrossRef](#)]

13. Mu, Z.; Guo, W.; Li, Y.; Tagawa, K. Wind tunnel test of ice accretion on blade airfoil for wind turbine under offshore atmospheric condition. *Renew. Energy* **2023**, *209*, 42–52. [[CrossRef](#)]
14. Anderson, D. Methods for scaling icing test conditions. In Proceedings of the 33rd Aerospace Sciences Meeting and Exhibit, Reno, NV, USA, 9–12 January 1995.
15. Jin, J.Y.; Virk, M.S. Study of ice accretion along symmetric and asymmetric airfoils. *J. Wind Eng. Ind. Aerodyn.* **2018**, *179*, 240–249. [[CrossRef](#)]
16. Zhu, Z.; Zhang, X.; Zhao, Y.; Huang, X.; Yang, C. Freezing characteristics of deposited water droplets on hydrophilic and hydrophobic cold surfaces. *Int. J. Therm. Sci.* **2022**, *171*, 107241. [[CrossRef](#)]
17. Tembely, M.; Dolatabadi, A. A comprehensive model for predicting droplet freezing features on a cold substrate. *J. Fluid Mech.* **2019**, *859*, 566–585. [[CrossRef](#)]
18. Zhang, X. Research on Freezing and Impact Processes of Supercooled Water Droplet and Their Coupling Characteristics. Ph.D. Thesis, Tsinghua University, Beijing, China, 2019. (In Chinese)
19. Enríquez, O.R.; Marín, G.; Winkels, K.G.; Snoeijer, J.H. Freezing singularities in water drops. *Phys. Fluids* **2012**, *24*, 091102. [[CrossRef](#)]
20. Fang, W.-Z.; Zhu, F.; Tao, W.-Q.; Yang, C. How different freezing morphologies of impacting droplets form. *J. Colloid Interface Sci.* **2021**, *584*, 403–410. [[CrossRef](#)]
21. Boinovich, L.B.; Emelyanenko, A.M. Recent progress in understanding the anti-icing behavior of materials. *Adv. Colloid Interface Sci.* **2024**, *323*, 103057. [[CrossRef](#)]
22. Carpenter, K.; Bahadur, V. Saltwater icephobicity: Influence of surface chemistry on saltwater icing. *Sci. Rep.* **2015**, *5*, 17563. [[CrossRef](#)]
23. Boinovich, L.B.; Emelyanenko, A.M.; Emelyanenko, K.A.; Maslakov, K.I. Anti-icing properties of a superhydrophobic surface in a salt environment: An unexpected increase in freezing delay times for weak brine droplets. *Phys. Chem. Chem. Phys.* **2016**, *18*, 3131–3136. [[CrossRef](#)] [[PubMed](#)]
24. ISO 12494; Atmospheric Icing of Structures. International Organization for Standardization: Geneva, Switzerland, 2017.
25. Singha, S.K.; Das, P.K.; Maiti, B. Influence of Salinity on the Mechanism of Surface Icing: Implication to the Disappearing Freezing Singularity. *Langmuir* **2018**, *34*, 9064–9071. [[CrossRef](#)] [[PubMed](#)]
26. Bauerecker, S.; Ulbig, P.; Buch, V.; Vrbka, L.; Jungwirth, P. Monitoring Ice Nucleation in Pure and Salty Water via High-Speed Imaging and Computer. *J. Phys. Chem. C* **2008**, *112*, 7631–7636. [[CrossRef](#)]
27. Vrbka, L.; Jungwirth, P. Brine Rejection from Freezing Salt Solutions: A Molecular Dynamics Study. *Phys. Rev. Lett.* **2005**, *95*, 148501. [[CrossRef](#)] [[PubMed](#)]
28. Carignano, M.; Baskaran, E.; Shepson, P.; Szleifer, I. Molecular dynamics simulation of ice growth from supercooled pure water and from salt solution. *Ann. Glaciol.* **2006**, *44*, 113–117. [[CrossRef](#)]
29. Zhang, Z.; Jin, L.; Yuan, Z.; He, S. The seawater surface tension coefficient representation with different salinities. *J. Exp. Fluid Mech.* **2017**, *31*, 45–50. (In Chinese)
30. Şahin, A.Z. An experimental study on the initiation and growth of frost formation on a horizontal plate. *Exp. Heat Transf.* **1994**, *7*, 101–119. [[CrossRef](#)]
31. Huang, W. The Experimental Determination and Prediction of Freezing Point of Salt-Water Systems. Master's Thesis, Xinjiang University, Urumqi, China, 2015. (In Chinese)

Disclaimer/Publisher's Note: The statements, opinions and data contained in all publications are solely those of the individual author(s) and contributor(s) and not of MDPI and/or the editor(s). MDPI and/or the editor(s) disclaim responsibility for any injury to people or property resulting from any ideas, methods, instructions or products referred to in the content.